5. L. N. Vlasova, S. G. Andreev, and M. M. Boiko, "Acceleration of a rigid piston by a stepped load," Tr. Mosk. Vyssh. Tekh. Uchil., No. 413 (1984).
6. V. S. Solov'ev, S. G. Andreev, et al., "Launching and loading of plates by detonation products in the implementation of overexpanded detonation regimes," Fiz. Goreniya Vzryva, No. 2 (1984).
7. R. Courant and K. O. Friedrichs, Supersonic Flow and Shock Waves, Wiley, New York (1948).
8. L. N. Vlasova and V. S. Solov'ev, "A case of quasiisentropic compression of a medium," Fiz. Goreniya Vzryva, No. 2 (1983).

SHOCK COMPRESSION OF POROUS MATERIALS

Yu. A. Krysanov and S. A. Novikov

UDC 675.532.620.178.7

Porous materials (sintered metal powders and foamed plastics) are complex mechanical structures. When loaded by shock waves to the point where their strength properties manifest themselves they display certain characteristic peculiarities.

The study of foamed polystyrene performed in [1] showed the presence of two steady-state shock waves followed by a nonsteady-state plastic compression wave. Upon motion of the two-wave system through the specimen the shock wave amplitude and velocity remain constant, depending solely on the relative density of the polystyrene. A similar complex structure with two steady-state shock waves has been observed in specimens of sintered copper powder [2, 3].

Using a unified methodological approach the present study will analyze experimental results for foamed polystyrene [1] and a number of sintered metals: copper, aluminum, tungsten, and beryllium [4-20]. Various methods exist for deriving analytical expressions to describe the mechanical characteristics of the porous material as functions of the relative density d, which is equal to the ratio of the porous material density to the density of the matrix material. For example, use has been made of theoretical studies of composite materials containing inclusions of close to spherical form, since vanishing of the elastic characteristics of the inclusions permits extending the results of such studies to porous materials. In [4-9] the elastic characteristics of composition materials were studied using the variation principles of the linear theory of elasticity. Estimates of elastic moduli were obtained using various models of the porous material structure. Of those studies we must take special note of [9], which obtained analytical expressions for the shear modulus and volume compression of porous materials, the use of which permits one to determine speed of propagation of oscillations in an infinite porous medium.

In [10] the dependence of the relative density of parts formed from metal powder upon pressing pressure was presented in the form of a power function. This approach was used later in [11, 12]. Various mechanisms for cell wall deformation in foamed plastic dependent on relative density were noted in [13].

We will represent the isotropic porous body in the form of a set of elementary cells, the boundaries of which are shown by dashed lines in Fig. 1. Such a representation is most obvious for bodies of the foamed plastic type. Sintered powders will be considered to consist of particles having acoustical contact and forming cells of the type shown in Fig. 1. Elastic perturbations propagate along some winding path formed by the elementary cell surfaces (solid line of Fig. 1). We introduce the following notation: v_0, mean size of an individual pore; N, number of pores per unit volume of the porous body; v_1, mean volume of an elementary cell of the porous body; v_2, volume of solid material in the porous body elementary cell. We will note that $v_2 = \lim v_1$ as $v_0 \to 0$. If we represent the porous body in the form of a cube of unit volume, then $v_0 = (1 - d)/N$, $v_1 = 1/N$, $v_2 = (1 - Nv_0)/N = d/N$.

Moscow. Translated from Zhurnal Prikladnoi Mekhaniki i Tekhnicheskoi Fiziki, No. 6, pp. 57-61, November-December, 1988. Original article submitted September 22, 1987.

 0021-8944/88/2906-0814 $12.50

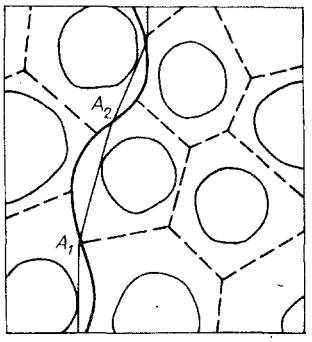

Fig. 1

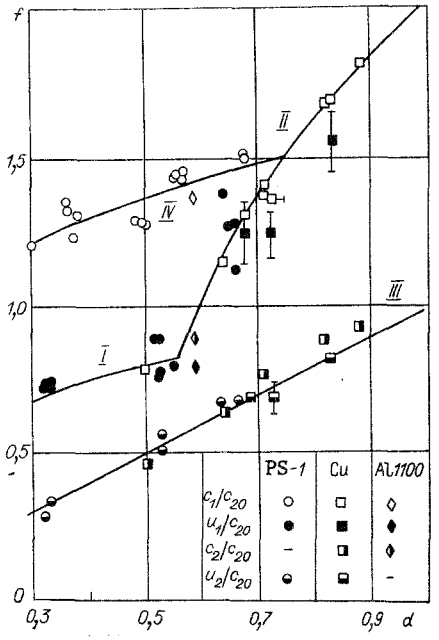

Fig. 2

The total surface area of the porous body elementary cells $S = Nv_1^{2/3} = N^{1/3}$ (here and below numerical factors determined by choice of cell shape are not considered since they drop out of the calculation process).

Along an arbitrary straight line in the porous body the ratio of the total length of line segments passing through solid material to the linear size of the specimen in that direction is equal to the relative density. If the number of intersections of the straight line with elementary cells $n = d/v_2^{1/3} = d^{2/3} N^{1/3}$ then the area of one such surface $S_2 = S/n = d^{-2/3}$. The mean path length for perturbation propagation in the porous body is then $\bar{l} = S^{1/2} = d^{-1/3}$ and the propagation speed along the mean path is $c = c_0 d^{1/3}$ (where c_0 is the speed of perturbation propagation in the solid material). The characteristic loading time for the experiments analyzed below was of the order of magnitude of several microseconds, i.e., the wavelength was several millimeters, significantly more than the thickness of the bridges joining elementary cells of the porous material cells. Therefore effects due to dispersion of the perturbation propagation speed were neglected. If we consider the shortest path h for propagation of weak perturbations (the segment A_1A_2) then $hv_0^{1/3} = d(1 - d)^{-1}$. Further $= [h^2 + (v_1^{1/3} - v_0^{1/3})^2]^{1/2}$, $h/\bar{l} = \{1 + d^{-2}(1 - d)^{4/3}[1 - (1 - d)^{1/3}]^2\}^{-1/2}$, or with consideration of the fact that $\bar{l} = d^{-1/3}$, $h = d^{-1/3}\{1 + d^{-2}(1 - d)^{4/3}[1 - (1 - d)^{1/3}]^2\}^{-1/2}$. The perturbation propagation rate over the shortest path can then be written with the expression $c = c_0 d^{1/3}\{1 + d^{-2}(1 - d)^{4/3}[1 - (1 - d)^{1/3}]^2\}^{-1/2}$.

The estimates made above are valid only for geometrically similar volumes v_0 and v_1, which is the case for porous bodies with a low relative density. At high values of d the relationship thus obtained may be inapplicable.

A series of experiments with porous material specimens having initial densities in the range 100-780 kg/m^3 was performed in [1]. Specimens were loaded by a steel plate 0.4 cm thick, driven by detonation of a layer of explosive. Initial plate velocity varied from 40 to 120 m/sec. The shock wave system pressure profile was measured by piezoquartz pressure sensors. Processing of the experimental shock wave parameter values as functions of the relative density by the method of least squares showed that for foamed plastic with relative density $0 < d < 0.6$ the wave velocity, pressure, and mass velocity in the first shock wave (D_1, p_1, u_1) were describable by power functions

$$Ad^b = \begin{cases} D_1(d), \\ p_1(d), \\ u_1(d). \end{cases}$$

TABLE 1

Parameters of first and second shock waves	A	b	Parameters of first and second shock waves	A	b
D_1, m/sec	1170±50	0,34±0,02	D_2, m/sec	1180±49	1
p_1, MPa	68,6±2,8	1,84±0,03	p_2, MPa	127,3±11,2	1,91±0,07
u_1, m/sec	54±3	0,49±0,04			

Values of the coefficients A and b are presented in Table 1. Results of measurements of the wave speed and pressure in the second wave (D_2 and p_2) are also described by a similar function. It proved to be the case that within the limits of experimental uncertainty the mass velocity in the second wave u_2 was independent of the relative density (b = 0) and equal to 71 ± 9 m/sec.

The results of these studies can be used to analyze the available data on shock compression of other porous bodies such as sintered metal powders in the moderate pressure range. There exist a number of studies [14-20] which present results of experimental investigations of shock compression. The results obtained and data of other authors for sintered aluminum, copper, beryllium, and tungsten are presented in Figs. 2 and 3. The ordinate indicates the speeds of sound and the shock wave, referred to the speed of propagation of shear oscillations in the solid material f, while the abscissa indicates relative density d. The behavior of the elastic characteristics of the porous material, copper, and aluminum can be described by a single curve, since for them the ratio c_{10}/c_{20} is practically the same (Fig. 2).

Data for tungsten and beryllium are shown in Fig. 3. Curve I of these figures shows the function $f(d) = d^{1/3}$ and describes the change in dimensionless velocity of the first shock wave for $d < 0.6$, while curve II is the dependence of dimensionless velocity of propagation of longitudinal elastic stresses obtained from analytical expressions for the effective elastic moduli [14]; curve III is the function $f(d) = d$, which describes the change in dimensionless velocity of the second shock wave, and curve IV is the function $f(d) = d^{1/3}\{1 + d^{-2}(1 - d)^{4/3}[1 - (1 - d)^{1/2}]^2\}^{1/2}$ obtained above, which describes the change in dimensionless velocity of propagation of longitudinal ultrasonic oscillations.

A comparison of calculated and experimental results shows their good agreement. One can also see certain characteristics in the reaction of porous and sintered materials to shock loading.

The rate of propagation of longitudinal elastic oscillations is the maximum rate of perturbation propagation. The first shock wave has a velocity markedly lower at $d < 0.6$, and approaches the velocity of elastic oscillations at $d > 0.6$. The second shock wave was observed in the range d = 0.1-0.8, with its propagation velocity depending linearly on the relative density.

In [15], which determined the Hugoniot elastic limit and the yield point in porous aluminum at d = 0.58 under quasistatic compression, those values proved to be equal. Experimental data were lacking for high d values. There are some indications of the possibility of dependence of the elastic Hugoniot limit on loading rate in [12].

We will now turn to experimental data on ultrasound studies and quasistatic and shock loading of porous specimens of the aluminum alloy Al_2O_{24}, obtained by hot pressing of powder [21-23]. As was noted in [22], at the moment of pressing, annealing of the material occurs. Study of the annealing process in an analogous aluminum alloy has shown that on the particle boundaries layers of intermetallic inclusions are formed, which have a remarkable effect on the mechanical properties of the specimens. Thus the porous aluminum must be considered as a three-phase system (aluminum alloy, intermetallic inclusions, and empty space). Use of the results of [14] for the three-phase system is difficult, since information on the mechanical characteristics and volume content of the inclusions is indefinite. However, an attempt can be made to describe behavior of the porous Al_2O_{24} aluminum alloy within the framework of a two-phase system by using the fact that the intermetallic inclusions have the form of thin layers on the aluminum particle contact boundaries.

Experimental data for the Al_2O_{24} aluminum alloy are shown in Fig. 4. Also shown there for comparison are data for practically pure aluminum A1100 with specimens produced by

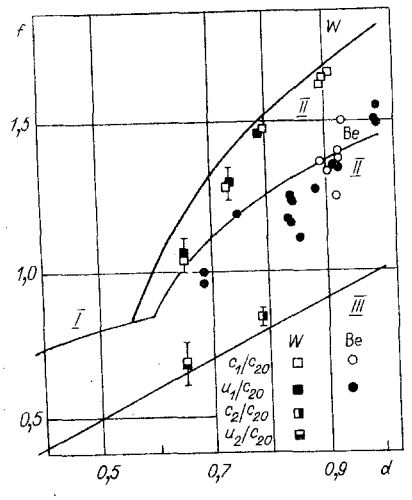

Fig. 3

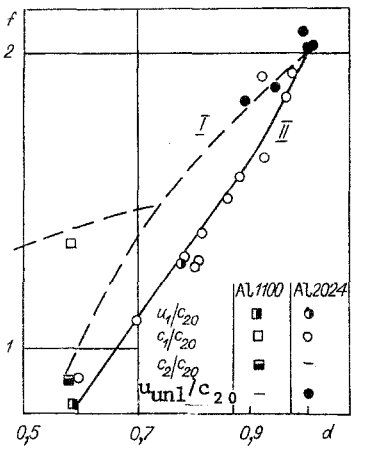

Fig. 4

the same technology [15]. As is evident from Fig. 4, to describe the dependence of longitudinal oscillation propagation rate on relative density it is necessary to take an effective rate of shear oscillation propagation equal to 2.3 km/sec (curve II). The following experimental fact indicates the existence of interlayers between the A12024 particles. The unloading wave propagation rate of 3.16 km/sec through the shock-compressed specimen agrees with curve I, obtained for the tabular value of shear oscillation propagation rate, which can be explained by destruction of the interlayers upon passage of the shock wave.

The role of intermetallic inclusions is especially obvious when the elastic characteristics of A11100 and A12024 specimens are compared at similar relative density values ($d \approx 0.6$). Although the propagation rates for longitudinal and shear oscillations in solid specimens of these materials are practically identical, the corresponding values for $d \approx 0.6$ differ greatly. It should also be noted that estimates of the dependence of longitudinal oscillation propagation rate on relative density calculated from the experimentally measured modulus of elasticity for quasistatic compression agree well with direct measurements.

It can be expected that the behavior of porous A120224 considered above is characteristic of porous multiphase materials with a similar impurity distribution. The comparison of behavior of porous materials and sintered metallic powders under shock loading presented above indicates that they follow one and the same principles.

LITERATURE CITED

1. S. I. Bodrenko, Yu. A. Krysanov, and S. A. Novikov, "Study of shock wave propagation in porous material," Zh. Prikl. Mekh. Tekh. Fiz., No. 6 (1979).
2. R. R. Boade, "Compression of porous copper by shock," J. Appl. Phys., 39, No. 12 (1968).
3. R. K. Linde, L. Seaman, and D. T. Schmidt, "Shock response of porous copper, iron, tungsten, and polyurethane," J. Appl. Phys., 43, No. 8 (1972).
4. B. Paul, "Prediction of elastic constants of multiphase materials," Trans. Met. Soc. AIME, 218, No. 2 (1960).
5. Z. Hashin, "The electic moduli of heterogeneous materials," J. Appl. Phys., 33, No. 2 (1962).
6. J. E. Mackenzie, "The elastic constants of solid containing spherical hobs," Proc. Phys. Soc. London B, 63, No. 2 (1950).
7. E. H. Kerner, "The elastic and thermo-elastic properties of composite media," Proc. Phys. Soc. London B, 69, No. 8 (1956).
8. R. M. Christensen, Mechanics of Composite Materials, Wiley-Interscience (1979).
9. B. Budiansky, "On the elastic moduli of some heterogeneous materials," J. Mech. Phys. Soc., 13, No. 4 (1965).
10. M. Yu. Val'shin, "Dependence of mechanical properties of powdered metals on porosity and failure properties of metalloceramic compounds," Dokl. Akad. Nauk SSSR, 67, No. 5 (1949).
11. B. I. Panshin, V. A. Popov, et al., "Mechanical properties of foamed plastics controlling their suitability as reinforcement fillers," Plast. Mass., No. 12 (1963).

12. P. S. Khuane, "Loss of strength in coarse porous bodies," Plast. Mass., No. 1 (1965).
13. M. Kats, "Modulus of elasticity of materials with a cellular-porous structure," Probl. Prochn., No. 3 (1972).
14. V. Herrman, "Equations of state for porous materials under compression," in: Problems in Structural Strength Theory, 7th Ed. [Russian translation], Mir, Moscow (1976).
15. J. R. Asay, "Shock and release behavior in porous 1100 aluminum," J. Appl. Phys., 46, No. 11 (1975).
16. R. R. Boade, "Dynamic compression of porous tungsten," J. Appl. Phys., 40, No. 9 (1969).
17. D. R. Dundekar and R. M. Lamothe, "Behavior of porous tungsten under shock compression at room temperature," J. Appl. Phys., 48, No. 7 (1977).
18. A. Buch and S. Goldschmidt, "Influence of porosity on elastic moduli of sintered materials," Mater. Sci. Engng., 4, No. 5 (1969/70).
19. G. Eden and C. R. Smith, "Elastic-plastic behavior of porous beryllium," in: Proc. 5th International Symposium on Detonation, Pasadena, California, 1970, Arlington (1970).
20. R. N. Schock, A. E. Aleg, and A. Duba, "Quasistatic deformation of porous beryllium and aluminum," J. Appl. Phys., 47, No. 1 (1976).
21. S. P. Marsh (ed.), LASL Shock Hugoniot data, Univ. California Press, Berkeley–Los Angeles–London (1980).
22. B. M. Butcher, M. M. Carroll, and A. C. Holt, "Shock wave compaction of porous aluminum," J. Appl. Phys., 45, No. 9 (1974).
23. B. M. Butcher, "Dynamic response of partially compacted porous aluminum during unloading," J. Appl. Phys., 44, No. 10 (1973).

MEASUREMENT OF HIGH ELECTRICAL CONDUCTIVITY IN SILICON IN SHOCK WAVES

S. D. Gilev and A. M. Trubachev

UDC 539.63:537.311.3

The study of dielectric (semiconductor)–metal phase transitions by measurement of electrical conductivity is of great interest in the physics of both shock waves and the solid state. The problem of conductivity measurement in a shock wave was formulated more than 20 years ago and has been considered by many authors [1-4]. The difficulties in solving this problem are related to the fact that under shock wave loading conditions the conductivity of the material changes by many orders of magnitude over a fraction of a microsecond, reaching values characteristic of classical metals. Measurement of conductivity under such conditions was considered in [5-11].

The most widely used measurement method is that involving a shunt connected in parallel with the specimen to be studied [5-9]. The shunt serves to couple the current to the power circuit and limits the range of change in voltage across the specimen. However, the spatial separation of the specimen and shunt leads to high inertia in the measurement circuit, which makes determination of high conductivity ($\sigma > 10^5\ \Omega^{-1}\cdot m^{-1}$) quite difficult. At present values in the range $\sigma \approx 10^4$-$10^5\ \Omega^{-1}\cdot m^{-1}$ can be recorded reliably.

The present study will offer an improved method for measurement of high conductivity together with a technique for processing the experimental data which insures nanosecond time resolution and raises the upper limit of measurable σ to 10^6-$10^7\ \Omega^{-1}\cdot m^{-1}$. The dependence of electrical conductivity on pressure will be determined for solid and porous silicon under conditions of single-time and multiple compression by shock waves in the intensity range 7-20 GPa.

1. Figure 1a shows the electrical circuit used for measurement of electrical conductivity during dielectric (semiconductor)–metal phase transitions. It includes a power supply (PS), shunt, and the specimen under study. At the initial moment the specimen resistance is high and practically all the current flows through the shunt. When the shock

Novosibirsk. Translated from Zhurnal Prikladnoi Mekhaniki i Tekhnicheskoi Fiziki, No. 6, pp. 61-67, November-December, 1988. Original article submitted September 23, 1987.

 0021-8944/88/2906-0818 $12.50